NANO LETTERS

2009
Vol. 9, No. 2
659-665

Nanoscale Oxidative Patterning of Metallic Surfaces to Modulate Cell Activity and Fate

Fiorenzo Vetrone,[†,‡,+] Fabio Variola,[†,‡,+] Paulo Tambasco de Oliveira,[†,§,+] Sylvia Francis Zalzal,[†] Ji-Hyun Yi,[†] Johannes Sam,[†] Karina F. Bombonato-Prado,[§] Andranik Sarkissian,[||] Dmitrii F. Perepichka,[⊥] James D. Wuest,[#] Federico Rosei,[‡] and Antonio Nanci*[,†]

Laboratory for the Study of Calcified Tissues and Biomaterials, Faculté de Médecine Dentaire, Université de Montréal, Montréal, Québec H3C 3J7, Canada, Institut National de la Recherche Scientifique - Énergie, Matériaux et Télécommunications, Université du Québec, Varennes, Québec J3X 1S2, Canada, School of Dentistry of Ribeirão Preto, University of São Paulo, 14040-904 Ribeirão Preto, São Paulo, Brazil, Plasmionique Inc., Varennes, Québec J3X 1S2, Canada, Department of Chemistry, McGill University, Montreal, Québec H3A 2K6, Canada, and Département de Chimie, Université de Montréal, Montréal, Québec H3C 3J7, Canada

Received October 7, 2008

ABSTRACT

In the field of regenerative medicine, nanoscale physical cuing is clearly becoming a compelling determinant of cell behavior. Developing effective methods for making nanostructured surfaces with well-defined physicochemical properties is thus mandatory for the rational design of functional biomaterials. Here, we demonstrate the versatility of simple chemical oxidative patterning to create unique nanotopographical surfaces that influence the behavior of various cell types, modulate the expression of key determinants of cell activity, and offer the potential of harnessing the power of stem cells. These findings promise to lead to a new generation of improved metal implants with intelligent surfaces that can control biological response at the site of healing.

Advances in nanotechnology underpin new and exciting research with applications in regenerative medicine, particularly in the area of biocompatible materials. Smart materials now being developed not only can incorporate themselves in the body but can also interact in predetermined ways with their host.[1] The biocompatibility of an implanted material is determined primarily by its initial interactions at the tissue/implant interface.[2] Several surface properties can affect these interactions, including composition, surface energy, roughness, and topography.[3,4] How these fundamental surface features determine biological activity is an important question that is just beginning to be answered. With proper control and management, manipulation of surface features may hold the key to developing innovative materials that not only are easily accepted by the human body but can have a subsequent functional effect.

Titanium (Ti) and its alloys are common biomaterials that are widely used in orthopedic, dental, and cardiovascular implants for multiple reasons. Most importantly, their native surface layer of inert amorphous TiO_2 confers excellent biocompatibility.[5] Surface modifications by techniques such as sandblasting,[6−8] machining,[9−11] and chemical treatment with acids[12,13] have been used successfully to modify topography at the microscale and to thereby stimulate cellular and tissue response. However, such modifications are not on the scale at which cells function. More recently, attention has focused on nanoscale surface modifications to improve biointegration, such as by creating specific nanogeometries that selectively influence and control cellular behavior.[14] On the horizon lies the advent of new intelligent nanostructured biomaterials with improved functionality, which is likely to benefit the health sector substantially.

* Author to whom all correspondence should be addressed: Antonio Nanci, P.O. Box 6128, Station Centre-Ville, Montreal, QC H3C 3J7. Tel: +1 (514) 343-5846. Fax: (514) 343-2233. E-mail: antonio.nanci@umontreal.ca.
† Laboratory for the Study of Calcified Tissues and Biomaterials, Faculté de Médecine Dentaire, Université de Montréal.
‡ Institut National de la Recherche Scientifique - Énergie, Matériaux et Télécommunications, Université du Québec.
§ School of Dentistry of Ribeirão Preto, University of São Paulo.
|| Plasmionique Inc.
⊥ Department of Chemistry, McGill University.
Département de Chimie, Université de Montréal.
+ These authors all contributed equally.

10.1021/nl803051f CCC: $40.75
Published on Web 01/21/2009

Chemical patterning is a versatile and powerful way to create functionalized nanostructured surfaces, with and without superimposed microtopography. Most earlier work has focused on nanoscale bumps, protrusions, and other features created by techniques such as anodization,[15,16] lithography (both photolithography and electron-beam lithography),[17−19] polymer demixing,[20] phase separation,[21] and evaporation.[22] Irrespective of the exact morphology of the features, nanostructuring has proven to have highly promising effects on the activity of cells, which are known to respond by modulating their adhesion, proliferation, migration, and gene expression.[23]

Recently, our group demonstrated the use of chemical oxidation to create reproducible nanopatterns on the surface of commonly used biocompatible metals such as Ti and Ti alloys.[24−28] By simply immersing the Ti-based material in an etching solution made by mixing concentrated sulfuric acid (H_2SO_4, a strong acid) and aqueous hydrogen peroxide (H_2O_2, an oxidant), it is possible to create a reproducible spongelike network of nanopits on the surface. These surfaces have been shown to have beneficial effects on both initial and subsequent osteogenic (bone-forming) events in vitro.[24−26]

The rationale for using H_2SO_4/H_2O_2 to nanotexture metals was to permit simultaneous etching and oxidation of the surface in a controlled manner.[29] This method is effective, but the range of nanoporosity achieved so far is narrow. In this paper, we introduce five new bicomponent reagents for nanotexturing, which extend the range of surface modifications that can be achieved by simple chemical oxidative etching. These novel etchants were applied to various implantable metals, and the physicochemical properties of the diverse nanogeometries created were characterized. We have also investigated how nanoscale physical cuing generated by surface texture modulates key determinants of cell activity. The versatility of oxidative chemical nanopatterning should make it possible to exert an influence on a broad spectrum of cell types (including stem cells) that play key roles in maintaining and restoring tissue structure and functional integrity.

We systematically varied the acidity/basicity of the etchants by examining the behavior of mixtures containing trifluoromethanesulfonic (triflic) acid (CF_3SO_3H), sulfuric acid (H_2SO_4), trifluoroacetic acid (CF_3COOH), and ammonium hydroxide (NH_4OH). Simultaneously, we studied the effect of various oxidants, including hydrogen peroxide (H_2O_2), *tert*-butyl hydroperoxide ($(CH_3)_3COOH$), and ammonium persulfate ($(NH_4)_2S_2O_8$). Using these new etchants, we were able to create diverse nanogeometries on the surface of biocompatible materials (Figure 1 and Figure S1 in Supporting Information). For example, neat CF_3SO_3H, which is orders of magnitude more acidic than H_2SO_4, was combined with 30% aqueous H_2O_2 as the oxidant. The effect of this mixture on Ti was to produce a spongelike network of nanopores similar to the one obtained with the H_2SO_4/H_2O_2 etchant (compare panels a and b of Figure 1 and S1). Using a weaker fluorinated acid, CF_3COOH, in conjunction with 30% aqueous H_2O_2, gave a distinct nanopattern consisting of nonuniform patches of nanopores extending across the surface (Figure 1c). A basic oxidative etchant consisting of concentrated aqueous NH_4OH and 30% aqueous H_2O_2 also proved to be very effective in nanopatterning the surface of Ti. This etchant mixture resulted in a nanopattern exhibiting large pits ranging in diameter between 50 and 100 nm. The morphology of the pits differed markedly from those obtained using acidic etchants; in particular, they appeared to be shallower and possessed irregular polygonal shapes. Furthermore, raising the percentage of peroxide in the etchant mixture resulted in a corresponding increase of the pit diameter.

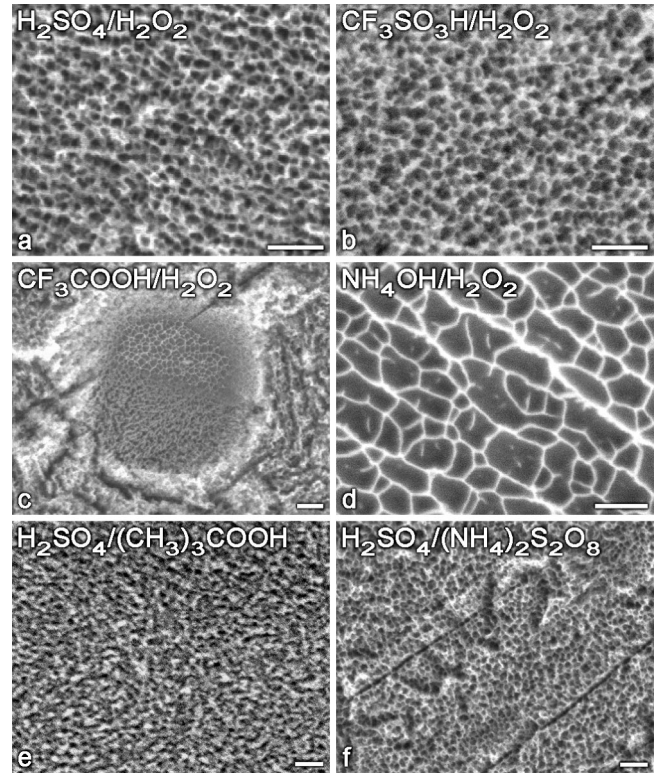

Figure 1. Characteristic SEM images of Ti surfaces nanostructured by oxidative etching under conditions specified in the experimental section (scale bar = 100 nm).

These results show that varying the acidic (or basic) component in mixtures containing H_2O_2 appreciably changes the nanopattern on Ti surfaces. We also studied a series of etchants with concentrated H_2SO_4 as the acidic component but with varied oxidants, and we compared Ti surfaces produced by exposure to these mixtures with the well-characterized nanostructured surfaces obtained by using the standard H_2SO_4/H_2O_2 mixture.[28] For example, a 50% v/v mixture of concentrated H_2SO_4 and water, mixed with equal volumes of $(CH_3)_3COOH$, produced a nanotexture consisting of pits and protrusions (Figure 1e). In addition, Ti disks exposed to mixtures of H_2SO_4 and $(NH_4)_2S_2O_8$ showed surfaces with microscale elevations and the smallest nanopits produced by any of the etchants tested (Figure 1f).

The novel nanostructured surfaces obtained by controlled chemical oxidation were subjected to detailed physicochemical characterization. Atomic force microscopy confirmed that the surfaces exhibited different roughness profiles (root mean

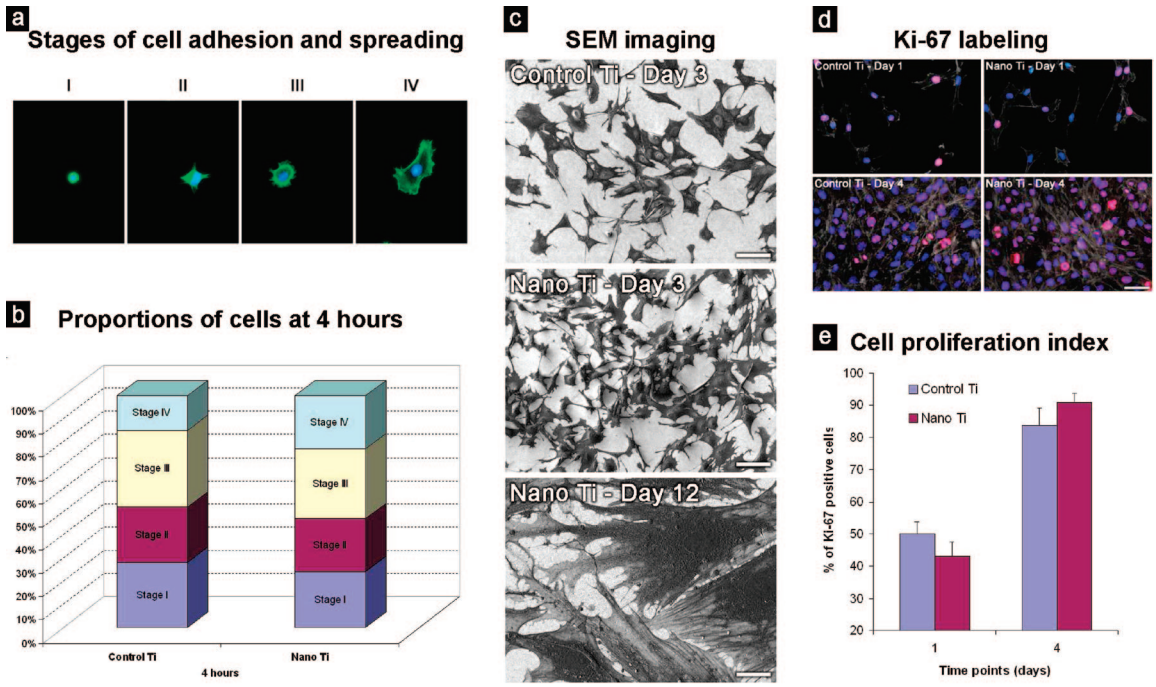

Figure 2. Comparative cell spreading number and proliferation profile of primary calvaria-derived osteogenic cells grown on control and nanotextured Ti surfaces. (a) Stages of cell adhesion and spreading as visualized by epifluorescence of phalloidin (actin cytoskeleton) and DAPI (nuclei) staining. (b) Proportions of cells in stages I−IV at 4 h postplating. (c) SEM images of cell spreading at days 3 and 12. (d) Triple-labeled preparations with an anti-Ki-67 antibody (red fluorescence), phalloidin, and DAPI, showing the distribution of cycling cells. (e) Cell proliferation index at days 1 and 4. Scale bars: (c) upper, center = 100 μm; lower = 25 μm; (d) = 50 μm.

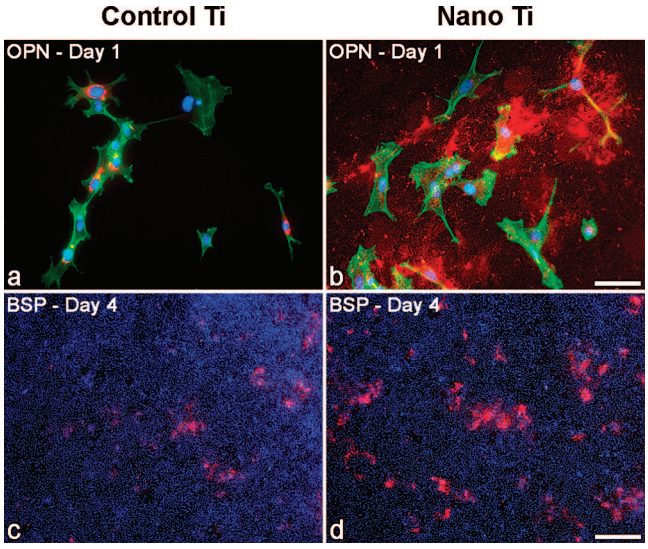

Figure 3. Immunolocalization of the matricellular proteins osteopontin (OPN) and bone sialoprotein (BSP) at early time points in primary calvaria-derived osteogenic cells grown on control (a, c) and nanotextured Ti surfaces (b, d). Note an expressive enhancement of the extracellular accumulation of OPN at day 1 and BSP at day 4 for the nanostructured Ti surface. Scale bar: upper = 50 μm; lower = 800 μm.

square values in the range of 10−200 nm on 5 × 5 μm^2 and 5−15 nm on 1 × 1 μm^2 scan areas), which is in agreement with the observation of various surface morphologies by scanning electron microscopy (Figure S1, Supporting Information). The crystallinity of the oxide layer of the newly obtained nanosurfaces was assessed by X-ray diffraction. No peaks corresponding to either rutile or anatase phases of TiO_2 were observed in the diffraction patterns of any samples, including untreated polished controls. This indicates that the chemical nanopatterning process does not alter the amorphous nature of the native TiO_2 layer. In all cases, the diffraction patterns showed only peaks corresponding to α-Ti.[30] On the other hand, Fourier-transform infrared (FTIR) spectra (Figure S2a, Supporting Information) revealed an overall thickening of the TiO_2 layer, as seen from the increase in the intensity of the peak in the Ti−O bond region (600 and 800 cm^{-1}) for nanosurfaces obtained by using CF_3SO_3H/H_2O_2, CF_3COOH/H_2O_2, and $H_2SO_4/(NH_4)_2S_2O_8$ as etchants. In sharp contrast, Ti surfaces treated with NH_4OH/H_2O_2 and $H_2SO_4/(CH_3)_3COOH$ mixtures yielded FTIR spectra that resembled those of untreated controls. We conclude that immersion of Ti in these two mixtures leads to the creation of oxide layers similar in thickness to the native layer. X-ray photoelectron spectroscopy (XPS) confirmed the FTIR data and identified TiO_2 as the major surface species in all samples studied. The Ti 2p core-level spectra showed the characteristic doublet at 458.6 eV (Ti $2p_{3/2}$) and 464.3 eV (Ti $2p_{1/2}$) attributed to Ti^{4+}, the oxidation state in TiO_2. In the case of untreated controls and of samples etched with NH_4OH/H_2O_2 and $H_2SO_4/(CH_3)_3COOH$, in which the oxide layer is relatively thin, a Ti^{metal} peak arising from the underlying metal was also detected (Figure S2b, Supporting Information).

Previously, we have shown that treating Ti with H_2SO_4/H_2O_2 removes surface contaminants and does not introduce S from the H_2SO_4 etchant.[29] However, XPS data revealed that S can be incorporated in nanopatterned Ti surfaces when $H_2SO_4/(NH_4)_2S_2O_8$ is used as the etchant. The presence of S

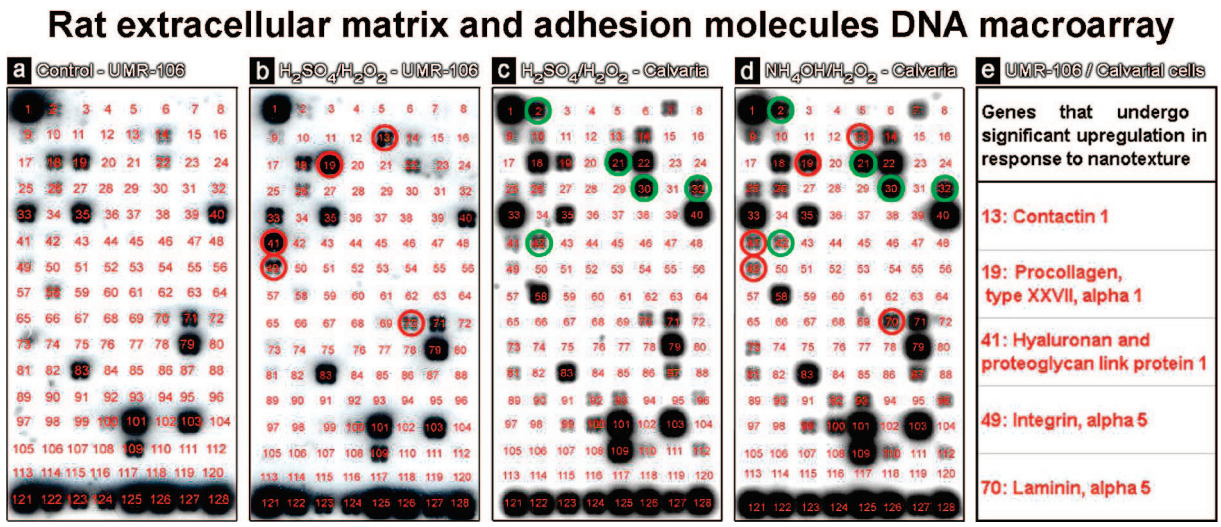

Figure 4. Macroarray analysis of gene expression for extracellular matrix and cell adhesion molecules by transformed UMR-106 (a, b) and primary calvaria-derived osteogenic cells (c, d) grown for 3 days on a control polished Ti surface (a) and on nanotextured surfaces obtained by etching with H_2SO_4/H_2O_2 (b, c) and with NH_4OH/H_2O_2 (d). Nanotexture upregulates expression of certain genes implicated in cell adhesion and migration (e, red circles in b and d). Green circles denote genes expressed by calvarial but not UMR-106 cells, highlighting the difference between primary and transformed cells.

on the surface may have favorable effects on the growth and repair of bone. The S dopant may yield $CaSO_4$ in the presence of tissue fluids, which is used in medicine as a filler that promotes repair of osseous defects.[31] Furthermore, samples treated with etchants containing fluorinated acids can also be doped with small amounts of trace elements such as F. This element is used commercially to improve osseointegration[32] and is known to have bactericidal activity. F-doped nanotextured surfaces prepared in this way may not only be advantageous for improving bone integration of implants, but their ability to control bacterial adhesion and proliferation may lead to other medical applications in the future.[33]

In addition to Ti, other metals and alloys are currently in wide use in implantable medical devices, including tantalum (Ta) and chromium cobalt molybdenum alloy (CrCoMo). By selecting the appropriate etchant and varying temperature, we found that simple chemical oxidative treatment was also effective for various metals (Figure S3, Supporting Information). These data suggest that suitable conditions can be found to nanotexture all implantable medically relevant metals, using oxidative patterning and appropriate choice of temperature, concentration, and other experimental parameters.

An important focus of our work has been on the effect that novel nanoporous surfaces produced by oxidative etching can have on osteoblastic cells (bone) and fibroblastic cells. Successful integration of an implant in bone depends on the relative growth of these two cell types. Stimulation of osteoblastic activity is essential for accelerating bone formation, and inhibition of fibroblastic cell growth is necessary to prevent formation of a fibrous capsule surrounding the implant, which weakens the bone−implant interface and can ultimately lead to failure.[34] In a recent report, we have shown that Ti alloy surfaces, when nanostructured using the standard H_2SO_4/H_2O_2 mixture, can promote the proliferation of essential osteoblastic cells and simultaneously inhibit the growth of unwanted fibroblastic cells.[25] We have now taken this observation further by comparing the effect of two distinct surfaces obtained by oxidative patterning on gene expression, cell adhesion, division, and differentiation.

Oxidative etching of Ti changes the physical characteristics of the surface, as well as its chemistry. We expected the combined effect of these alterations to influence cells in contact with the surface. Cell culture studies revealed that controlled nanopatterning has a series of interesting and unexpected effects. In particular, we found that treatment of Ti surfaces with H_2SO_4/H_2O_2 alters the adhesion, spreading dynamics, and growth of primary osteogenic cells. At 30 min following plating, the cells exhibited a rounded appearance, and there were more adherent cells on nanostructured Ti than on untreated controls (data not shown). After 4 h of culture, there was no significant difference in the number of cells, but there was a significant increase in the proportion of cells that had a spread morphology on the nanoporous surface (stage IV, Figure 2a,b).[35] After 3 days, there were more cells on the treated surface, as revealed by scanning electron microscopy (SEM), and after 12 days they showed well-developed cellular processes with focal adhesions at the extremities (Figure 2c). Labeling for the nuclear protein Ki-67, a marker for the cell division cycle,[36] showed that at day 1 there were more Ki-67 positive cells on untreated control Ti, but at day 4 a significant increase in the number of cycling cells on nanotextured Ti was detected. The differential in proliferative index from day 1 to day 4 was about 120% for the nanostructured surface and only 67% for the unetched control (Figure 2d,e). Extracellular accumulation of osteopontin (OPN) and bone sialoprotein (BSP), two major bone matrix proteins,[37,38] increased dramatically on the nanoporous Ti surface (Figure 3). Taken together, these data indicate that osteogenic differentiation is accelerated, and they also suggest that proteins are retained or adsorbed more efficiently on the nanopatterned surface.

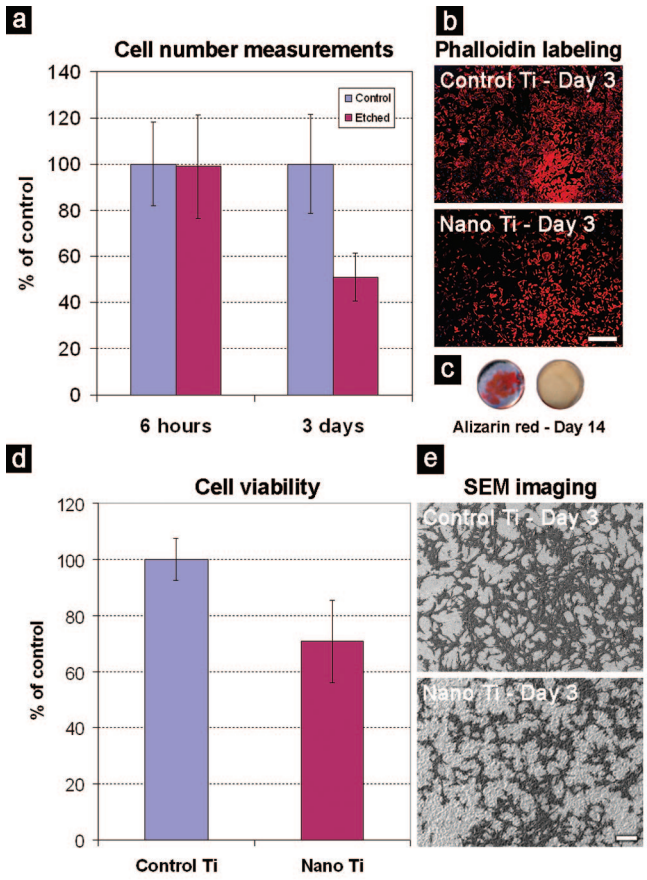

Figure 5. (a−c) Cell growth profiles of MC3T3-E1 osteogenic cells grown on untreated Ti surfaces and on surfaces etched with NH_4OH/H_2O_2. The surface features generated by this treatment limit cell growth and the development of the osteogenic phenotype. Scale bar = 500 μm. (c) At 14 days of culture, Alizarin red staining for mineral reveals abundant areas of calcification on the control surface (left disk), but none is detected on the treated surfaces (right disk). (d, e) Cell growth profile of NIH3T3 fibroblastic cells grown on untreated Ti surfaces and on surfaces etched with NH_4OH/H_2O_2. (d) Evaluation of cell number by the MTT viability test. (e) SEM image. These data show that surface features generated by this treatment limit the growth of fibroblastic cells. Scale bar = 100 μm.

Gene profiling using whole genome DNA microarrays has recently been used to elucidate the molecular mechanisms implicated in cellular response to nanomodified surfaces.[39] Because such surfaces elicit broad gene responses, we have opted to use chips that screen for limited gene sets associated with extracellular matrix and cell adhesion molecules. For surfaces etched with either H_2SO_4/H_2O_2 or NH_4OH/H_2O_2, genes associated with cell adhesion and migration (such as integrin alpha-5 and hyaluronan) were significantly upregulated, irrespective of the cell type screened (Figure 4).

Unlike etching Ti with H_2SO_4/H_2O_2, treatment with NH_4OH/H_2O_2 creates nanoporosity without increasing the thickness of the native oxide layer. After 6 h of culture, there was no significant difference between MC3T3-E1 osteogenic cell growth on NH_4OH/H_2O_2-treated surfaces and on controls, indicating that the surface modifications have no effect on cell adhesion (Figure 5a). After 3 days, however, there were significantly fewer cells on the treated surface than on the control, suggesting that etching retards growth of the cell population (Figure 5a,b). This reduction in cell growth leads to less mineral deposition after 14 days, as visualized by staining with Alizarin red (Figure 5c). The growth of NIH3T3 fibroblastic cells, measured at 3 days, is also significantly reduced following surface nanostructuring with NH_4OH/H_2O_2 (Figure 5d,e). Future work will determine whether the distinctly different cellular responses to the two oxidative treatments (H_2SO_4/H_2O_2 and NH_4OH/H_2O_2) arise from differences in nanotexture, thickness of the oxide layer, or both. Subsequent studies of cellular growth on Ti treated with $H_2SO_4/(CH_3)_3COOH$, which creates a nanotexture similar to that obtained with H_2SO_4/H_2O_2 but does not thicken the native oxide layer, should help resolve the individual contributions of the two parameters.

The striking ability of NH_4OH/H_2O_2 to inhibit cell growth creates attractive opportunities. For example, the key challenge in developing improved stents for cardiovascular medicine is to control excessive cell growth, which eventually leads to the restenosis of vessels. An important feature of our work is its demonstration that such selective cellular generates controlled of nanotopography, with or without microtexture or changes in the thickness of the native oxide layer.

Harnessing the power of stem cells is a major challenge that promises breakthroughs in many areas of regenerative medicine. Physical characteristics of the extracellular matrix have been shown to be important in stem cell lineage specification,[40] and there is now growing evidence that nanoscale surface features can also guide their differentiation.[41] Stem cells are not abundant in adult tissues, and the ability to promote their expansion would be highly beneficial. Our studies show that nanoporous surfaces created by chemical oxidation accelerate the growth of human umbilical cord stem cells when compared with untreated Ti and glass coverslips (Figure 6). The physicochemical cuing provided by such surfaces increases expression of Ki-67, a marker of cell proliferation. In addition, ongoing studies show that nanoporosity upregulates expression of alkaline phosphatase by umbilical cord stem cells, at least when grown in osteogenic medium (data not shown). This suggests that nanoporosity also has an effect on cell differentiation.

In conclusion, our results support the concept that physical cues emanating from surfaces can influence cells, much like biochemical signals. Moreover, our work establishes that sophisticated signaling can be achieved by a simple chemical oxidation. As stated by Ingber,[42] it is now increasingly recognized that cells are governed by the same architectural principles that define the nonliving natural world, reaffirming the importance of integrating chemistry and physics into cell biology. At present, however, we still do not understand in detail how nanostructured surfaces exert their effects, and there are no simple ways to predict what influence a particular nanoscale surface modification will have on cells. Cellular distortion is well-known to cause reorganization of the cytoskeleton and to trigger various signaling pathways that are involved in determining the fate and morphogenesis of cells.[43] Signal transduction pathways that have been

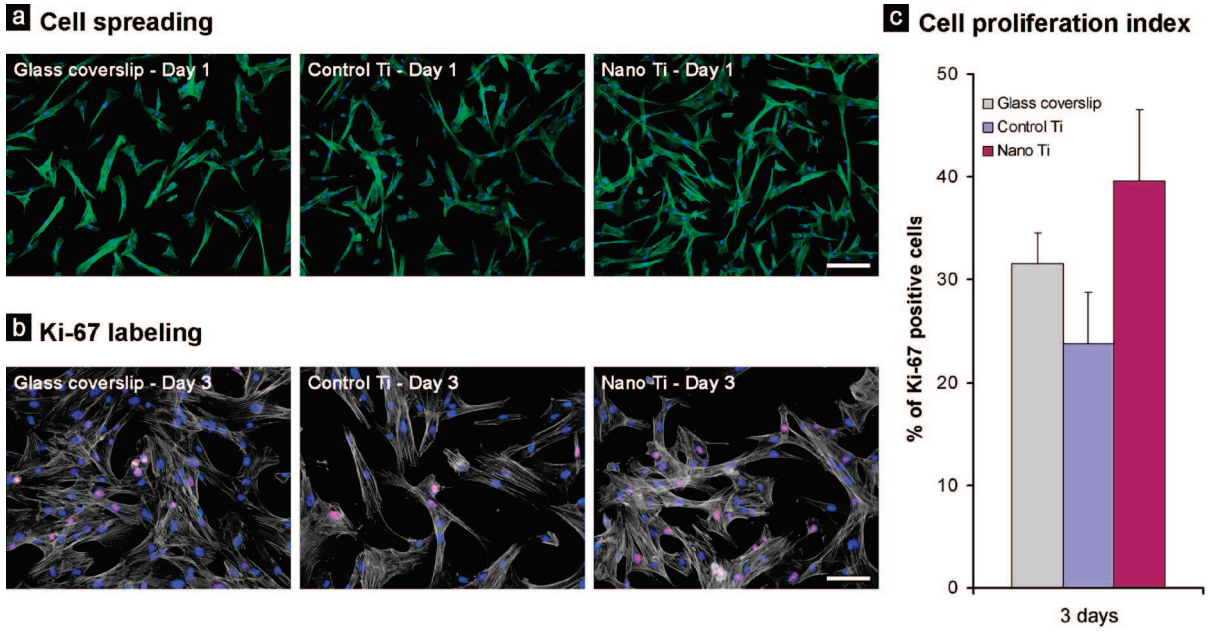

Figure 6. Human umbilical cord (HUC)-derived cells grown on control Ti surfaces, nanotextured Ti surfaces, and on control glass coverslips. (a) At day 1, HUC cells were well spread on all surfaces, exhibiting an elongated shape. Areas of higher cell density were frequently observed for nanostructured Ti. (b, c) Dual nuclear labeling with an anti-Ki-67 antibody (red fluorescence) and DAPI (blue fluorescence) at day 3 allowed the detection of significantly more cycling cells on nanotextured Ti compared to controls (1.6-fold increase compared to control Ti). Phalloidin labeling appears green in (a) and pale white in (b). Scale bar = 200 μm (a) and 100 μm (b).

implicated in these activities include Rho GTPase, ERK MAP, and Src kinase. In addition, physical interactions between cells and extracellular matrix modulate formation of stress fibers and focal adhesion complexes. In a similar manner, nanostructured substrates may induce nanoscale cellular distortions that sum up and cumulatively produce enough strain to induce cytoskeletal reorganization, changes in cell shape, and the triggering of various signaling pathways. Upregulation of genes such as contactin-1, hyaluronan, and integrin-α_5 observed in our macroarrays certainly suggests an important effect on cell shape, motility, and Rho intracellular signaling. However, the subject is complex, and it remains necessary to correlate well-defined surface characteristics with specific cellular effects. This complexity is illustrated by a recent comparison of the effects of periodic arrays of nanopores created by electron-beam lithography with those of disorganized arrays of the same nanopores, which showed that the haphazard arrangement was better for stimulating the differentiation of human mesenchymal stem cells into osteogenic cells.[39] Consistent with this observation, the nanoporosity generated by our methods of chemical oxidation does not exhibit any apparent order. Previous studies have addressed the issues of surface chemistry, roughness, and morphology, but only on the microscale. The conclusion of these studies is that the beneficial influence of microtopography on osteogenic cell activity actually results from chemical modification of the surface rather than from topographic cuing.[6] It must also be noted that surface modifications also affect the adsorption of proteins, which then secondarily alters cellular activity.[44] Whether such effects arise from nanoscale features remains to be determined and will require additional studies. Nevertheless, it is likely that surface morphology and chemistry will act in concert, and a better understanding of these parameters and their interrelation is mandatory for the rational design of novel biomaterials. Learning how these parameters determine the behavior of relatively simple inorganic biomaterials such as metals provides an excellent starting point for developing deeper knowledge of other families of materials that are widely used in regenerative medicine, such as polymers.

Acknowledgment. We acknowledge funding from the Canadian Institutes of Health Research (CIHR) and the Natural Sciences and Engineering Research Council of Canada (NSERC) through a Collaborative Health Research Project grant. In addition, we thank NSERC for a Collaborative Research and Development grant with Plasmionique, Inc. (Varennes, QC, Canada). A.N. also acknowledges funding from the CIHR and the Canada Foundation for Innovation. F.R. is grateful to the Fonds québécois de la recherche sur la nature et les technologies (FQRNT) and for start-up funds from INRS. F.R. and J.D.W. acknowledge support from the Canada Research Chairs Program and from NSERC (Discovery Grants). P.T.O. is grateful to the São Paulo State Research Foundation (FAPESP) for research funding and thanks graduate student Larissa M. Spinola de Castro (U. São Paulo at Ribeirão Preto, Brazil) for helping with cell adhesion and proliferation experiments. The mouse monoclonal anti-rat osteopontin (MPIIIB10-1) and anti-rat bone sialoprotein (WVID1-9C5) antibodies, developed by Michael Solursh and Ahnders Franzen, were obtained from the Developmental Studies Hybridoma Bank formed under the auspices of the NICHD and maintained by The University of Iowa, Department of Biological Sciences (Iowa City, IA 52242). F.Ve. is grateful for a postdoctoral fellowship from

NSERC, and F.Va. acknowledges the Canadian Bureau for International Education (CBIE) and FQRNT for financial support. The authors kindly thank Karine Sellin and Rima Wazen for their assistance with cell culture.

Supporting Information Available: (1) Detailed experimental section, (2) additional information on etchants, (3) Fourier-transform infrared spectroscopy, (4) AFM topographies of nanostructured Ti surfaces, (5) FTIR and XPS spectra, and (6) AFM topographies of nanostructured Ti surfaces. This material is available free of charge via the Internet at http://pubs.acs.org.

References

(1) Anderson, J. M. *J. Mater. Sci.: Mater. Med.* **2006**, *17*, 1025.
(2) Puleo, D. A.; Nanci, A. *Biomaterials* **1999**, *20*, 2311.
(3) Boyan, B. D.; Lohmann, C. H.; Dean, D. D.; Sylvia, V. L.; Cochran, D. L.; Schwartz, Z. *Annu. Rev. Mater. Res.* **2001**, *31*, 357.
(4) Brunski, J. B.; Puleo, D. A.; Nanci, A. *Int. J. Oral Maxillofac. Implants* **2000**, *15*, 15.
(5) Williams, D. F. In *Biocompatibility of Clinical Implant Materials*; CRC Series in Biocompatibility; CRC Press: Boca Raton, FL, 1981; Vol. 5.
(6) Anselme, K.; Bigerelle, M. *J. Mater. Sci.: Mater. Med.* **2006**, *17*, 471.
(7) Guizzardi, S.; Galli, C.; Martini, D.; Belletti, S.; Tinti, A.; Raspanti, M.; Taddei, P.; Ruggeri, A.; Scandroglio, R. *J. Periodontol.* **2004**, *75*, 273.
(8) Refai, A. K.; Textor, M.; Brunette, D. M.; Waterfield, J. D. *J. Biomed. Mater. Res., Part A* **2004**, *70*, 194.
(9) Cassinelli, C.; Morra, M.; Bruzzone, G.; Carpi, A.; Di Santi, G.; Giardino, R.; Fini, M. *Int. J. Oral Maxillofac. Implants* **2003**, *18*, 46.
(10) Lüthen, F.; Lange, R.; Becker, P.; Rychly, J.; Beck, U.; Nebe, J. G. B. *Biomaterials* **2005**, *26*, 2423.
(11) Xavier, S. P.; Carvalho, P. S. P.; Beloti, M. M.; Rosa, A. L. *J. Dent.* **2003**, *31*, 173.
(12) Bagno, A.; Di Bello, C. *J. Mater. Sci.: Mater. Med.* **2004**, *15*, 935.
(13) Sittig, C.; Textor, M.; Spencer, N. D.; Wieland, M.; Vallotton, P.-H. *J. Mater. Sci.: Mater. Med.* **1999**, *10*, 35.
(14) Balasundaram, G.; Webster, T. J. *J. Mater. Chem.* **2006**, *16*, 3737.
(15) Yao, C.; Webster, T. J. *J. Nanosci. Nanotechnol.* **2006**, *6*, 2682.
(16) Yao, C.; Slamovich, E. B.; Webster, T. J. *J. Biomed. Mater. Res., Part A* **2008**, *85*, 157.
(17) Ball, M. D.; Prendergast, U.; O'Connell, C.; Sherlock, R. *Exp. Mol. Pathol.* **2007**, *82*, 130.
(18) Diehl, K. A.; Foley, J. D.; Nealey, P. F.; Murphy, C. J. *J. Biomed. Mater. Res., Part A* **2005**, *75*, 603.
(19) Teixeira, A. I.; McKie, G. A.; Foley, J. D.; Bertics, P. J.; Nealey, P. F.; Murphy, C. J. *Biomaterials* **2006**, *27*, 3945.
(20) Barbucci, R.; Pasqui, D.; Wirsen, A.; Affrossman, S.; Curtis, A.; Tetta, C. *J. Mater. Sci.: Mater. Med.* **2003**, *14*, 721.
(21) Wan, Y.; Wang, Y.; Liu, Z.; Qu, X.; Han, B.; Bei, J.; Wang, S. *Biomaterials* **2005**, *26*, 4453.
(22) Cai, K.; Bossert, J.; Jandt, K. D. *Colloids Surf., B* **2006**, *49*, 136.
(23) Yim, E. K. F.; Leong, K. W. *Nanomedicine* **2005**, *1*, 10.
(24) de Oliveira, P. T.; Nanci, A. *Biomaterials* **2004**, *25*, 403.
(25) Richert, L.; Vetrone, F.; Yi, J.-H.; Zalzal, S. F.; Wuest, J. D.; Rosei, F.; Nanci, A. *Adv. Mater.* **2008**, *20*, 1488.
(26) de Oliveira, P. T.; Zalzal, S. F.; Beloti, M. M.; Rosa, A. L.; Nanci, A. *J. Biomed. Mater. Res., Part A* **2007**, *80*, 554.
(27) Variola, F.; Yi, J.-H.; Richert, L.; Wuest, J. D.; Rosei, F.; Nanci, A. *Biomaterials* **2008**, *29*, 1285.
(28) Yi, J.-H.; Bernard, C.; Variola, F.; Zalzal, S. F.; Wuest, J. D.; Rosei, F.; Nanci, A. *Surf. Sci.* **2006**, *600*, 4613.
(29) Nanci, A.; Wuest, J. D.; Peru, L.; Brunet, P.; Sharma, V.; Zalzal, S.; McKee, M. D. *J. Biomed. Mater. Res.* **1998**, *40*, 324.
(30) XRD Joint Committee on Powder Diffraction Standards (JCPDS) Data File No. 44-1294.
(31) Thomas, M. V.; Puleo, D. A.; Al-Sabbagh, M. *J. Long-Term Eff. Med. Implants* **2005**, *15*, 599.
(32) Cooper, L. F.; Zhou, Y.; Takebe, J.; Guo, J.; Abron, A.; Holmén, A.; Ellingsen, J. E. *Biomaterials* **2006**, *27*, 926.
(33) Yoshinari, M.; Oda, Y.; Kato, T.; Okuda, K. *Biomaterials* **2001**, *22*, 2043.
(34) Ratner, B. D.; Hoffman, A. S.; Schoen, F. J.; Lemons, J. E. In *Biomaterials Science; An Introduction to Materials in Medicine*; Academic Press: San Diego, 1996; Chapter 4.
(35) Rajaraman, R.; Rounds, D. E.; Yen, S. P. S.; Rembaum, A. *Exp. Cell. Res.* **1974**, *88*, 327.
(36) Scholzen, T.; Gerdes, J. *J. Cell Physiol.* **2000**, *182*, 311.
(37) Alford, A. I.; Hankenson, K. D. *Bone* **2006**, *38*, 749.
(38) Nanci, A. *J. Struct. Biol.* **1999**, *126*, 256.
(39) Dalby, M. J.; Gadegaard, N.; Tare, R.; Andar, A.; Riehle, M. O.; Herzyk, P.; Wilkinson, C. D. W.; Oreffo, R. O. C. *Nat. Mater.* **2007**, *6*, 997.
(40) Engler, A. J.; Sen, S.; Sweeney, H. L.; Discher, D. E. *Cell* **2006**, *126*, 677.
(41) Yim, E. K. F.; Pang, S. W.; Leong, K. W. *Exp. Cell. Res.* **2007**, *313*, 1820.
(42) Ingber, D. E. *Proc. Natl. Acad. Sci. U.S.A.* **2005**, *102*, 11571.
(43) Huang, S.; Ingber, D. E. *Nat. Cell Biol.* **1999**, *1*, E131.
(44) Stevens, M. M.; George, J. H. *Science* **2005**, *310*, 1135.

NL803051F